NASA TECHNICAL NOTE

NASA TN D-4202

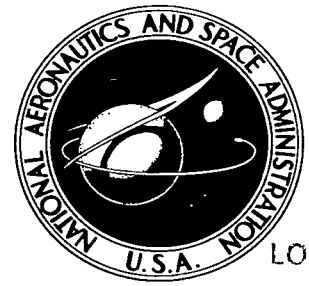

MECHANISM OF DEUTERON BREAKUP BY 42-MEV ALPHA PARTICLES

by Robert E. Warner and Robert W. Bercaw

Lewis Research Center
Cleveland, Ohio

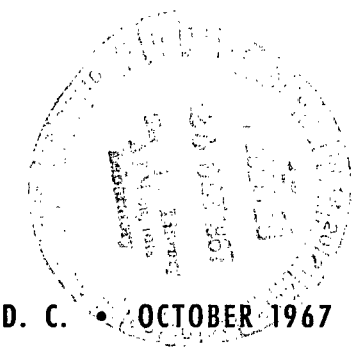

NATIONAL AERONAUTICS AND SPACE ADMINISTRATION • WASHINGTON, D. C. • OCTOBER 1967

NASA TN D-4202

MECHANISM OF DEUTERON BREAKUP BY 42-MEV ALPHA PARTICLES

By Robert E. Warner and Robert W. Bercaw

Lewis Research Center
Cleveland, Ohio

NATIONAL AERONAUTICS AND SPACE ADMINISTRATION

For sale by the Clearinghouse for Federal Scientific and Technical Information
Springfield, Virginia 22151 – CFSTI price $3.00

MECHANISM OF DEUTERON BREAKUP BY 42-MEV ALPHA PARTICLES

by Robert E. Warner* and Robert W. Bercaw

Lewis Research Center

SUMMARY

Coincidence measurements of absolute cross sections for the breakup of deuterons by 42-MeV alpha particles have been made. The alpha-particle energy spectra show large peaks due to final-state interactions (FSI) through the helium 5 and lithium 5 ground states. Plane-wave impulse approximation calculations correctly predict the existence of additional peaks for small spectator neutron energies, but otherwise give bad fits to the observed spectra. In general, the yields in the spectator peaks exceed those in the FSI peaks. Especially large cross sections, approximately 1 barn per square steradian (100 fm^2/sr^2) (integrated over alpha energy), are observed when kinematic conditions are such that alpha plus proton can form the lithium 5 ground state, with the neutron left as a spectator. Analysis of the more prominent FSI peaks yields a binding energy and width of -0.88±0.12 and 0.75±0.20 MeV, respectively, for the ground state of helium 5; the corresponding figures for lithium 5 are -1.9 and 1.4 MeV.

INTRODUCTION

The alpha-particle induced breakup of the deuteron is one of the simplest three-body nuclear reactions and hence one of the most attractive for study. The following features of this reaction are of special interest: (1) it is the only inelastic channel open to the d-α system below the threshold for $\alpha+d \rightarrow {}^3H + {}^3He$, and, (2) it is influenced by final state interactions (FSI) in the unbound helium 5 and lithium 5 (^5He and ^5Li) ground states, and by the deuteron wave functions. Proton energy spectra for the reaction have been measured by Warburton and McGruer (ref. 1) and by Ohlsen and Young (ref. 2), who deduced the location and width of the ^5He ground state. More recently, Nagatani, Tombrello, and Bromley (ref. 3) have observed proton spectra from deuteron breakup

*NASA-ASEE Faculty Fellow, Summer, 1966. Permanent address: Oberlin College, Oberlin, Ohio.

by 29- and 42-MeV alpha particles. They observed a peak at the high energy end of the proton spectra attributable to the ^{5}He FSI. Some spectra also showed a broad peak at lower energies, probably resulting from the ^{5}Li FSI, but slightly displaced from the expected location and superimposed on a very large continuum.

There has not yet been a detailed comparison of the various theories of this reaction with experiment, partly because of a lack of particle-particle coincidence data. This report presents absolute cross sections for coincidence detection of α+p from this reaction. These data clearly show sharp peaks from both the ^{5}He and ^{5}Li FSI, and considerably broader spectator pole peaks arising from α+p quasi-electric scattering with the neutron kinetic energy remaining essentially equal to its initial value while bound in the deuteron. Very small yields are obtained under kinematic conditions such that neither can take place, and hence they are identified as the primary breakup mechanisms. An improved theoretical analysis of this reaction, in which FSI are taken into account and exact final-state wave functions are used, is now being completed by H. Nakamura of Aoyama Gakuin Univ., Tokyo, Japan (private communication); it is hoped that the present work provides a sufficiently complete set of experimental data to give a critical test of this new theoretical treatment.

SYMBOLS

C	half-height of detectors, cm
D	deuteron binding energy, MeV
d	deuteron
$\left(\frac{d\sigma}{d\Omega}\right)_{\alpha\text{-p}}$	differential cross section for α-p elastic scattering, mb/sr^2 - MeV; fm^2/sr^2 - MeV
$\frac{d^3\sigma}{d\Omega_\alpha d\Omega_p dE_\alpha}$	differential cross section for α-d breakup; mb/sr^2 - MeV; fm^2/sr^2 - MeV
E	5-mm diode of telescope used to detect protons
ΔE	0.2-mm diode of telescope used to detect protons
E_n	kinetic energy of final neutron, MeV
ΔE_n	increase in kinetic energy of neutron due to noncoplanarity, MeV
E_o	kinetic energy of incident alpha particle, MeV
E_p	kinetic energy of final proton, MeV

E_α kinetic energy of scattered alpha particle, MeV

$E_{\alpha n}$ relative energy of α+n in their center-of-mass systems

$E_{\alpha p}$ relative energy of α+p in their center-of-mass systems

E_1 1.113 MeV (parameter in Hulthen wave function)

E_2 29.9 MeV (parameter in Hulthen wave function)

L distance from target to detectors, cm

M 1-mm diode used as a monitor

N_d yield of recoil deuterons

N_I number of inelastic α-d breakup events detected during runs

N_M number of elastically scattered α particles detected by monitor counter during run

t half height of beam spot on target, cm

α 1-mm diode used to detect alpha particles

β N_d/N_M

β_α N_d/N_M ratio using alpha counter to detect deuterons

β_p N_d/N_M ratio using proton counter to detect deuterons

θ_α polar scattering angle of alpha particle

θ_p polar scattering angle of proton

$\theta_{\alpha p}$ included angle between momentum vectors of scattered alpha particle and proton

φ azimuthal angle between plane containing incident and scattered alpha-particle momentum vectors and plane containing incident alpha particle and recoil proton momentum vectors

$\Phi(p_n)$ Fourier transform of Hulthen deuteron wave function

$\Delta\Omega_p$ solid angle of proton detector

$\Delta\Omega_\alpha$ solid angle of alpha detector

Subscripts:

d deuteron

p proton

α alpha particle

EXPERIMENTAL PROCEDURE

The 42-MeV alpha-particle beam of the NASA Lewis cyclotron was analyzed and focused on a deuterated polyethylene (CD_2) foil target at the center of a 160-centimeter-diameter scattering chamber by the apparatus shown in figure 1. A beam spot about 2 millimeters wide and 1 centimeter high was obtained. The unscattered beam was collected by a Faraday cup. Deuteron breakup events were detected by observing coincidences between a 1-millimeter-lithium-drifted - alpha-particle detector and a two-counter proton telescope employing a 200-micrometer transmission ΔE counter and a 5-millimeter lithium-drifted E detector. The proton and alpha counters were located on opposite sides of the beam and their centers were coplanar with it. All detectors operated at dry-ice temperature. The solid angle $\Delta\Omega_\alpha$ subtended by the α counter was defined by a slit 0.304 centimeter wide by 0.635 centimeter high and 15.3 centimeters from the target center, while that of the proton telescope $\Delta\Omega_p$ was defined by an aperture of 0.638-centimeter diameter, 15.6 centimeters from the target center.

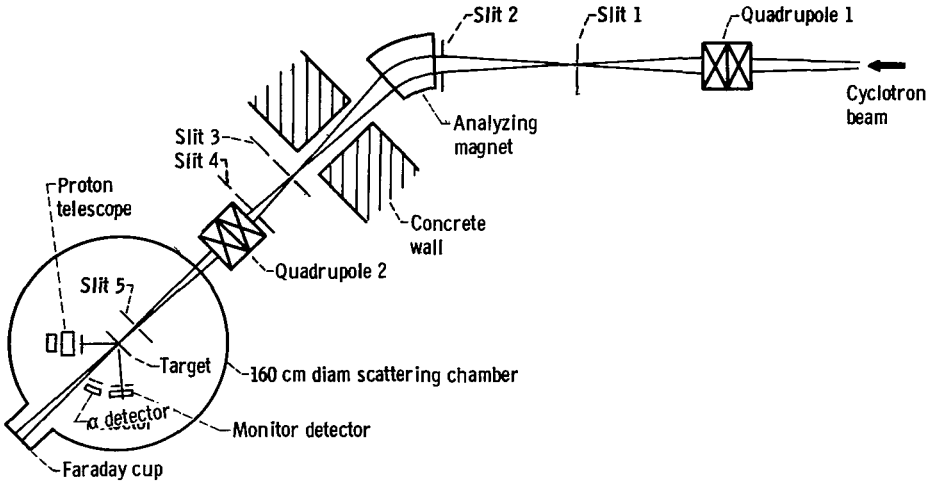

Figure 1. - Layout of cyclotron beam and scattering chamber.

A 1-millimeter monitor detector M, at 49° on the same side of the beam as the α counter, detected alpha particles from elastic α-carbon scattering.

A block diagram of the electronics used in the experiment is shown in figure 2. Signals from the three detectors were amplified in Goulding and Landis (ref. 4) pulse analysis boxes and then subjected to fast and slow coincidence and proton identification requirements. A fast coincidence (2τ = 100 nsec) was required between the crossover pickoff of the ΔE and α counters, but not the E counter, whose timing was energy dependent. A slow coincidence (2τ = 400 nsec) was then required between the fast output and the single channel analyzers on the α and E signals. Signals satisfying these requirements were then allowed to pass through linear gates for further analysis.

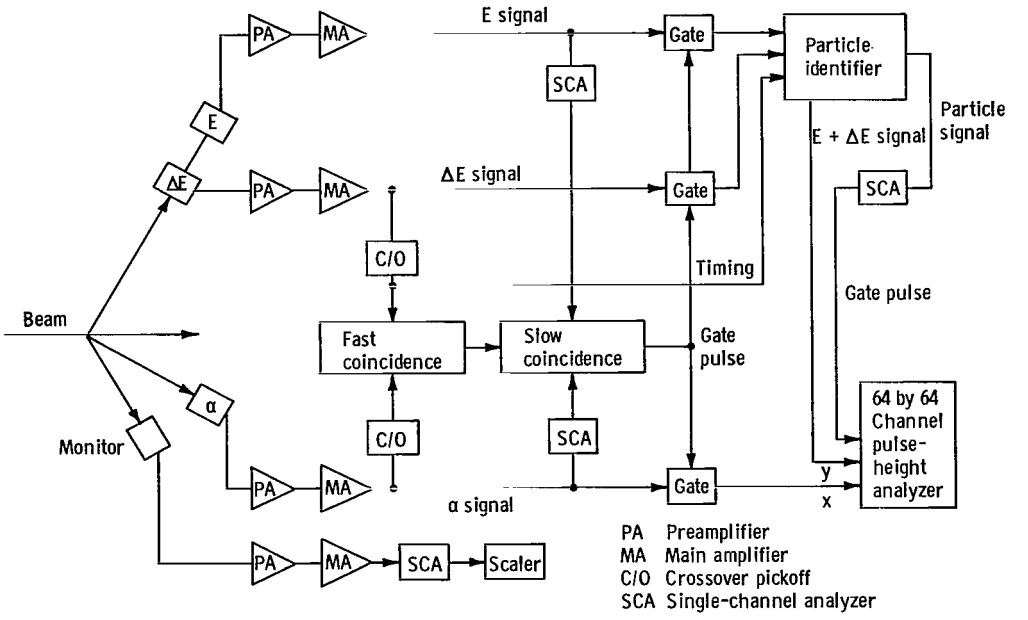

Figure 2. - Simplified electronics block diagram.

The signals from the proton detectors were added and presented to a Goulding (ref. 4) identifier circuit which produced a completely resolved mass spectrum. A single-channel analyzer set on the proton peak of this spectrum then allowed the α and $E + \Delta E$ signals to be recorded in a two dimensional pulse-height analyzer operated in a 64 by 64 channel mode. The proton energy threshold was approximately 5 to 6 MeV. The above requirements in conjunction with the kinematic relations between the proton and alpha energies were sufficient to eliminate background except that from α-p elastic scattering at some angles. This was subtracted, as is discussed later.

A number of equipment checks were made by coincidence detection of α-p elastic scattering from a thin CH_2 target. The fast coincidence was found to have an efficiency of 100 percent. Delay curves were measured for several scattering angles, and the maximum variation in the centers of delay curves for particle energies detected in this experiment was less than 10 nanoseconds. Finally, energy calibrations were obtained. The response was linear to better than 1 percent (integral), and the widths of the two-dimensional elastic peaks (typically 0.8 MeV full width at half-maximum) were largely accounted for by kinematic broadening due to the finite geometry of the apparatus. These checks as well as checks on the particle identifier were repeated throughout the course of the experiment, but no significant variations were observed.

In order to determine absolute cross sections for this reaction, it was necessary to repeatedly determine the deuterium content of the target, which decreased continuously because of radiation damage to the CD_2. This was done by measuring the yield of elastic recoil deuterons and deducing the deuterium areal density from the cross sections reported by Broek and Yntema (ref. 5) at this center-of-mass energy. Although it would

have been desirable to measure the elastic deuteron yield for each data run, an additional multichannel pulse-height analyzer was not available for the monitor counter. Instead, the yield of alphas elastically scattered by carbon at 49° was determined by the single-channel analyzer of the monitor counter. This yield N_M was then related to the yield of recoil deuterons N_d during the frequent measurements of the deuterium areal density. The ratio $\beta = (N_d/N_M)$ was measured using both the proton and alpha counters to detect the deuterons and the two values are designated β_p and β_α, respectively. We judge that the true value of β is known to better than 5 percent throughout the experiment because both β's as well as the ratio of the elastic deuteron yield to the charge collected in the Faraday cup varied smoothly and gradually as a function of the charge passed through the target. In addition, the inelastic cross section was measured twice for the same geometry at different times during the experiment. Although the β's differed by 35 percent, the results agreed to within 1 percent. The initial thickness of the target was measured with an alpha-particle gage and the initial yields of both deuterons from α-d scattering and alphas from α-carbon scattering were consistent with this thickness. Loss of deuterons caused the normalizing factor β to change by a factor of two during the experiment. The factors β as measured by the proton detector and the alpha detector should be related by the $\beta_p \Delta\Omega_\alpha = \beta_\alpha \Delta\Omega_p$, where $\Delta\Omega_\alpha$ and $\Delta\Omega_p$ are the solid angles of the two detectors; however, $\beta_p \Delta\Omega_\alpha$ was consistently 3 percent larger than $\beta_\alpha \Delta\Omega_p$. The average value was used in computing the inelastic cross sections.

The inelastic cross sections were determined from the formula

$$\frac{d^3\sigma(\theta_p, \theta_\alpha, E_p, E_\alpha)}{d\Omega_p d\Omega_\alpha dE_\alpha} = \frac{(d\sigma/d\Omega)_{\alpha,d}}{(\beta\,\Delta\Omega)\Delta E_\alpha} \frac{N_I}{N_M}$$

where N_I is the sum of α-d breakup events observed in the proton channels corresponding to one alpha-particle channel of energy width ΔE_α, N_M is the monitor count during the period of accumulation of inelastic data, and $(d\sigma/d\Omega)_{\alpha,d}$ is the elastic α-d cross section.

Deuteron breakup events were identified kinematically. Conservation of energy and linear momentum relate E_p and E_α through the following equations:

$$E_p^{1/2} = -A \pm \sqrt{A^2 - 0.5B}$$

where

$$A = E_\alpha^{1/2} \cos \theta_{\alpha p} - E_0^{1/2} \cos \theta_p$$

$$B = 5E_\alpha + 3E_0 + D - 8(E_0 E_\alpha)^{1/2} \cos \theta_\alpha$$

$$\cos \theta_{\alpha p} = \cos \theta_p \cos \theta_\alpha + \sin \theta_p \sin \theta_\alpha \cos \varphi$$

and E_0 and D are the kinetic energy of the incident alpha-particle and the deuteron binding energy, respectively. The polar scattering angles of the two detected particles are called θ_p and θ_α, and φ is the azimuthal angle between the plane containing the two alpha-particle momentum vectors and the plane containing the momentum vectors of the incident alpha particle and recoil proton (i.e., $\varphi = 180^\circ$ for the coplanar events detected in this experiment). A typical kinematic curve of E_p against E_α appears in figure 3; the solid curve applies to coplanar events in which the particles go to the detector center, and the cross hatching indicates the kinematic broadening due to finite detector and target size. In general, E_p is a double-valued function of E_α. Since the lower proton energy was always too low for such protons to be detected with perfect efficiency, the cross sections measured in this investigation were at the higher proton energy. For each run, a kinematic check was made at several α energies by noting

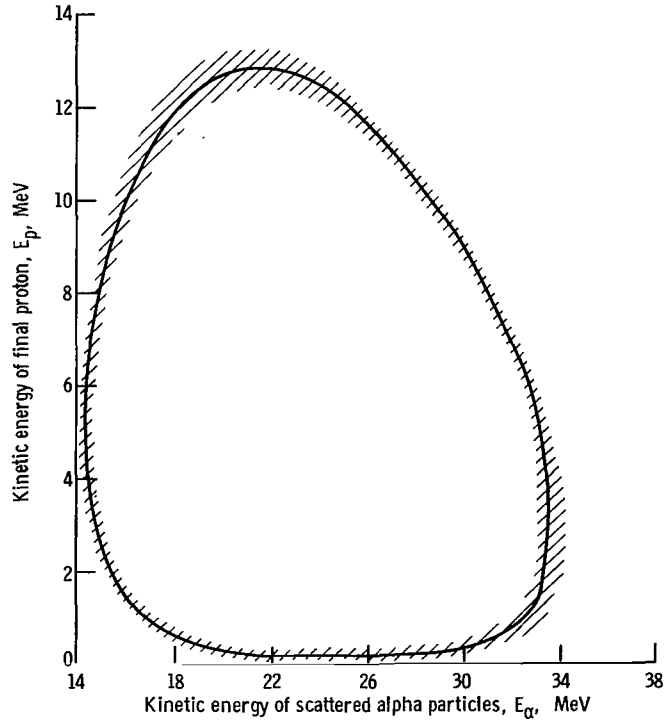

Figure 3. - Kinematic plot of energy of final proton as function of energy of scattered alpha particles. Scattering angle of alpha particle, 14.8°; scattering angle of proton, 60°.

that the proton channel containing the most counts was always within one channel of the channel corresponding to the calculated E_p. The number of inelastic events N_I at each E_α was found by adding the counts in the seven proton channels centered on the channel with the most counts; these channels (a 3-MeV interval) included all but a negligible fraction of the inelastic events.

Random coincidence rates were measured by delaying the ΔE crossover signal input to the fast coincidence circuit by one cyclotron period (90 nsec). Typical true to chance coincidence ratios varied from 0.01 in the peaks to 0.2 for the smallest inelastic cross sections. The principal nonrandom background was elastic α-p scattering from the 1 percent hydrogen contamination in the CD_2 target. For $(\theta_p, \theta_\alpha)$ equal to $(50^\circ, 14.8^\circ)$, $(30^\circ, 14.8^\circ)$, and $(20^\circ, 9.8^\circ)$, the included angle between counters was within 1.5° of the correlation angle for elastic α-p scattering, and the finite counter size caused elastic α-p peaks to be observed in the two-dimensional spectra. In other geometries, these angles differed by 3° or more, and no elastic peaks were seen. The centers of the three observed peaks were displaced in the $E_p - E_\alpha$ plane from the α-d breakup region, but they spilled down into this region. Therefore, the elastic α-p contaminations in the inelastic α-d spectra were subtracted by comparison with spectra from a 1-milligram-per square-centimeter self-supporting carbon target containing 30 percent hydrogen contamination. Carbon runs at these and several other geometries showed that the total cross section for breakup of carbon is less than 3 percent of the total inelastic cross sections, and no correction for this source of background has been made.

The true zero-degree location of the alpha counter was determined by measuring the alpha-carbon elastic cross section at small angles on both sides of the beam; it differed by 0.2° from the mechanical zero-degree location. The zero-degree location of the proton counter was determined optically. The second method is slightly less accurate, but both the energy calibration and the location of the peaks in the two-dimensional spectra are insensitive to the proton counter position.

The beam was centered vertically by measuring the dependence of the elastic α-p coincidence rate from a CH_2 target on the current in a vertical steering magnet, and running with the magnet current which produced the maximum rate.

DISCUSSION OF RESULTS

General

The absolute cross sections for this reaction for an alpha scattering angle of 9.8°

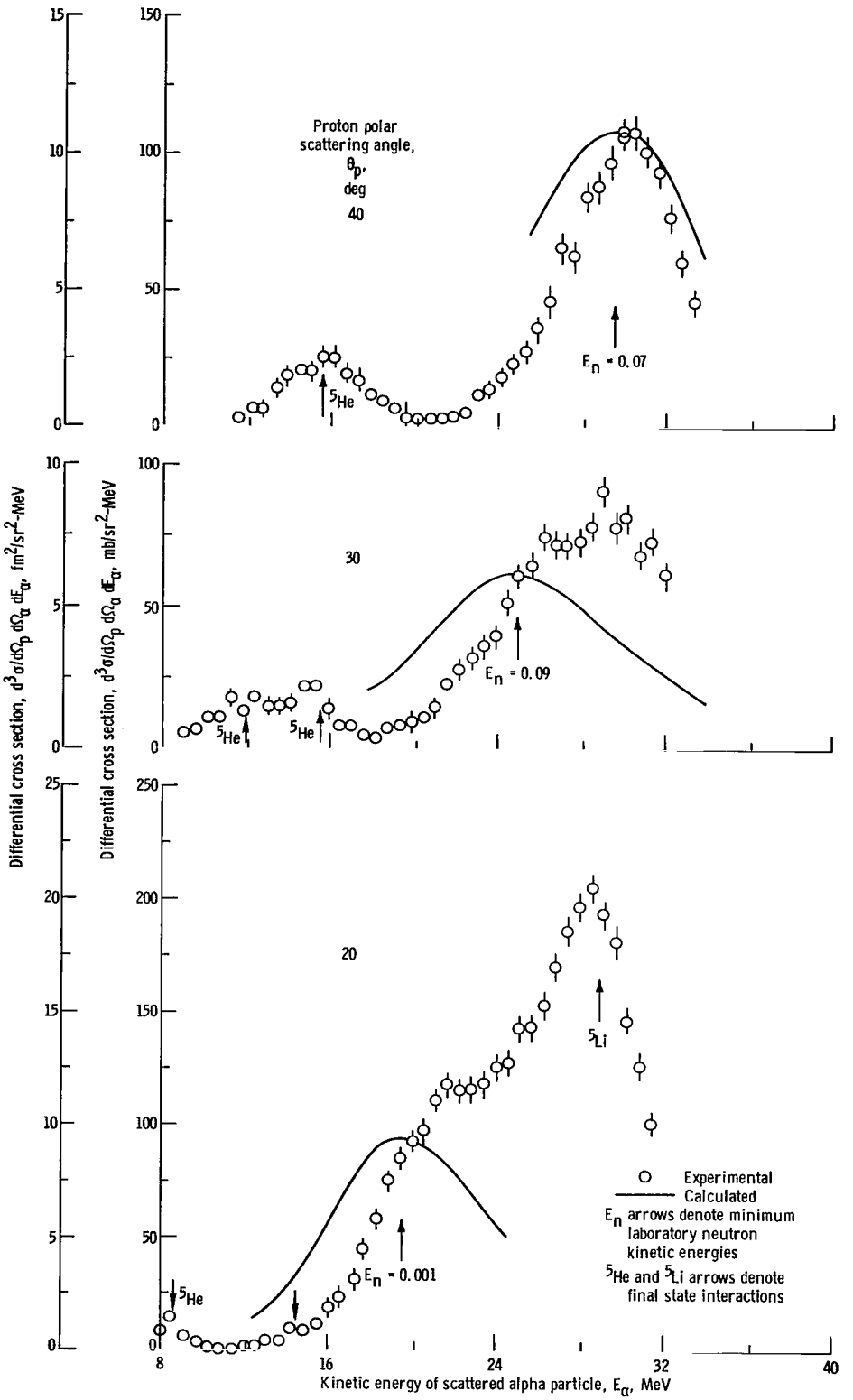

Figure 4. - Cross section of α - d breakup. Alpha particle polar scattering angle, 9.8°; deuteron breakup reaction, α + d → α + p + n. Calculated curves are normalized to measured cross sections at minimum neutron laboratory energies.

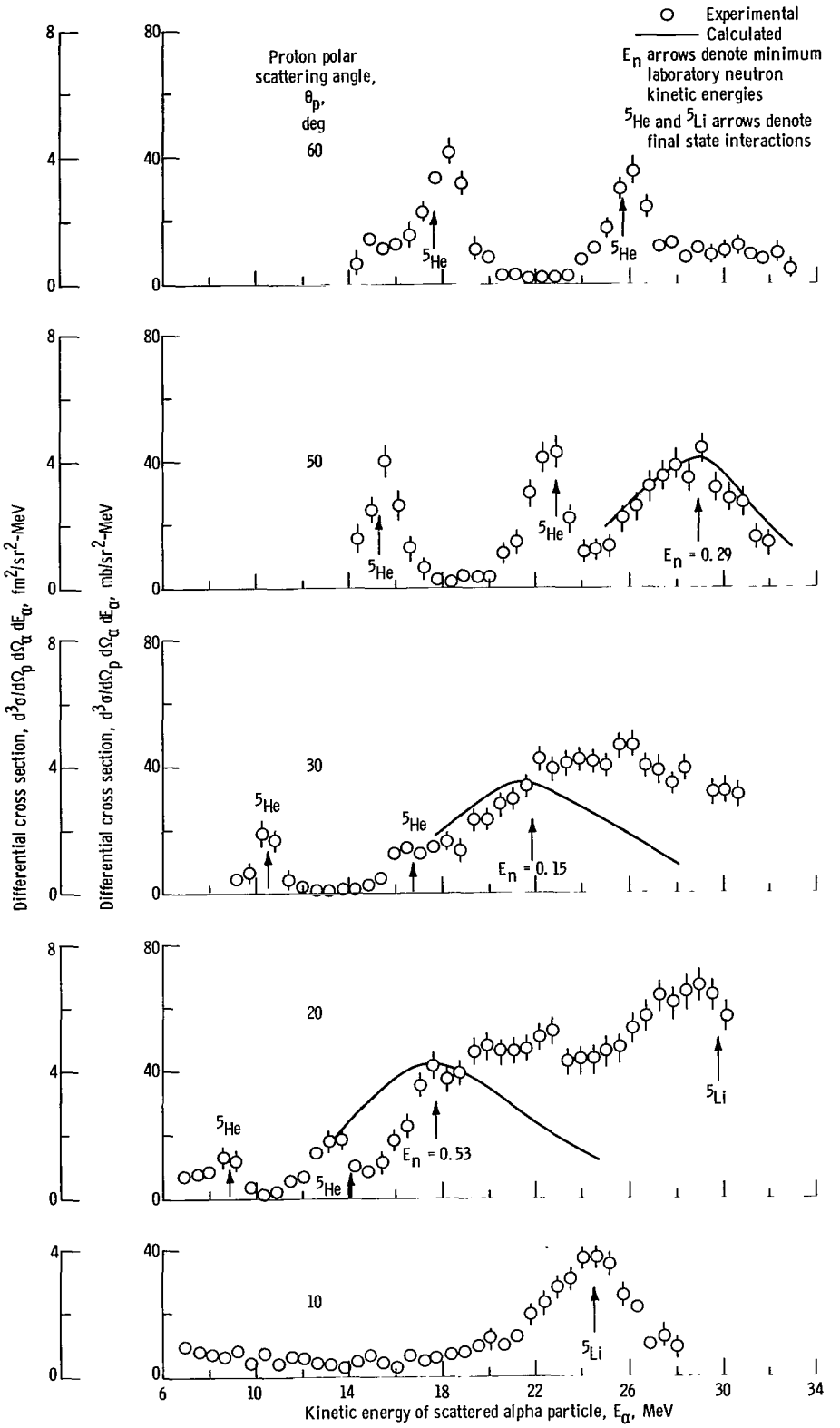

Figure 5. - Cross section of α - d breakup. Alpha-particle polar scattering angle, 14.8°; deuteron breakup reaction, α + d → α + p + n. Calculated curves are normalized to measured cross sections at minimum laboratory energies.

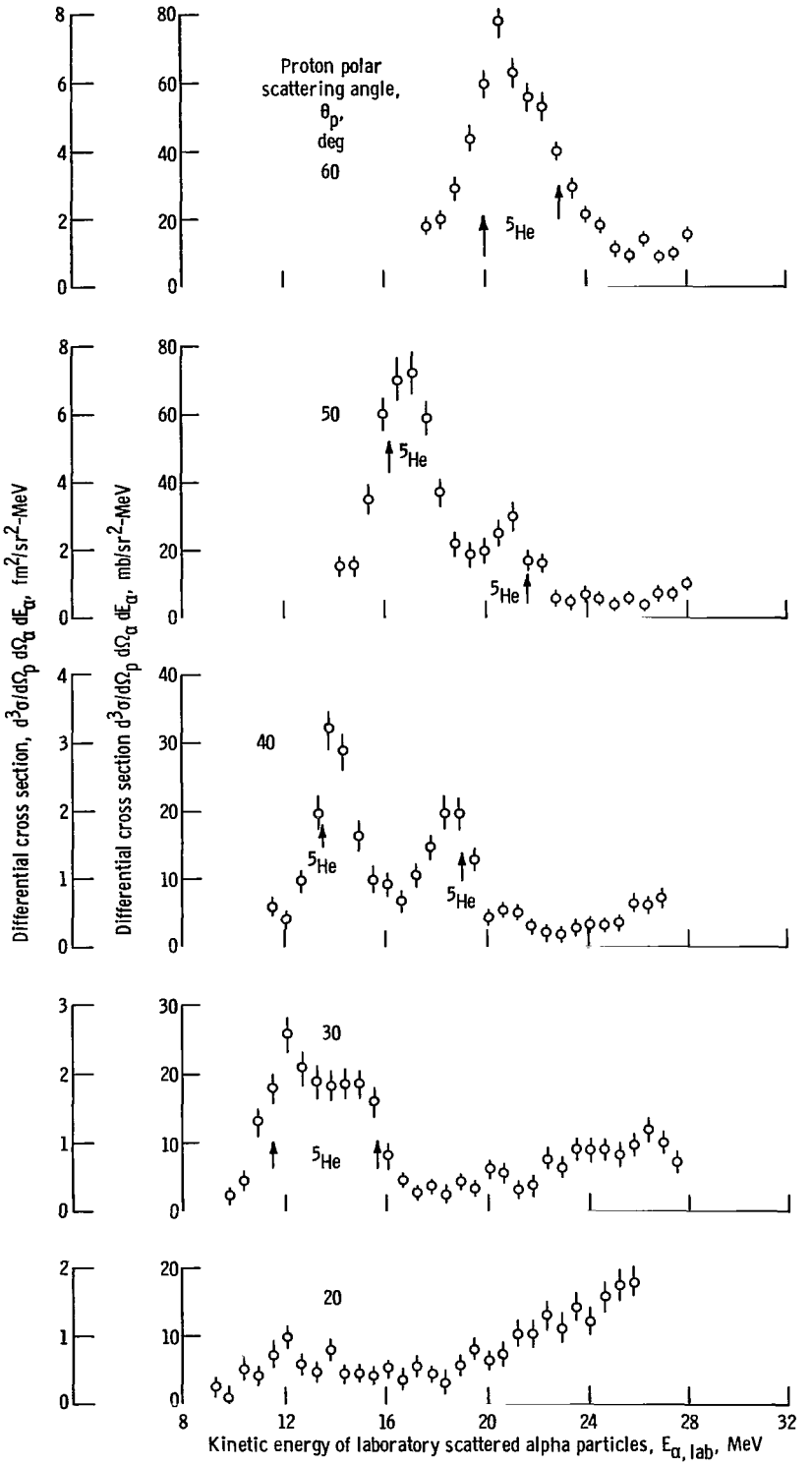

Figure 6. - Cross sections of α - d breakup. Alpha-particle polar scattering angle, 19.8°; scattering reaction, α + d → α + p + n.

and three different proton detection angles appear in figure 4. Likewise, data for $\theta_\alpha = 14.8^\circ$ and 19.8° appear in figures 5 and 6, respectively.

Plane-Wave Impulse Approximation Theory

Kuckes, Wilson, and Cooper (ref. 6) have given a simplified theoretical treatment of nucleon-deuteron breakup in which the following assumptions are made: The interaction of the incident nucleon with one of the nucleons in the deuteron is ignored, the deuteron ground state is described by a Hulthén wave function, and all unbound nucleons have plane-wave functions. The nucleon-nucleon elastic scattering cross section is calculated in Born approximation, and the elastic and inelastic cross sections are then related. This theory works fairly well at 150 MeV but not at lower energies. It has been adapted for alpha-deuteron breakup by Burress (ref. 7) who obtains the formula

$$\frac{d^3\sigma}{d\Omega_\alpha d\Omega_p dE_\alpha} = \frac{25E_p\sqrt{E_\alpha}\sqrt{E_1E_2}\left(\sqrt{E_1}+\sqrt{E_2}\right)^3 (d\sigma/d\Omega)_{\alpha\text{-}p}}{\pi^2\sqrt{2E_0}\left(\sqrt{E_p}+\sqrt{E_\alpha}\cos\theta_{\alpha p}-\sqrt{E_0}\cos\theta_p\right)(E_1+2E_n)^2(E_2+2E_n)^2}$$

where $(d\sigma/d\Omega)_{\alpha\text{-}p}$ is the measured center-of-mass α-p elastic differential cross section at the angle at which the momentum transfer to the alpha particle is the same as in the inelastic event under consideration. This theory gave bad fits, both in shape and in magnitude, to the observed spectra, and, in particular, the FSI peaks were not reproduced. However, it correctly predicted the existence, but not the magnitude, of broad spectator peaks, three of which are seen in figure 4. The physical interpretation of these is as follows: The two nucleons in the deuteron are very frequently outside the range of each other's nuclear forces, hence, breakup is very likely to occur by quasi-elastic scattering of the alpha-particle from only one nucleon. No momentum is transferred to the second nucleon (in this case, the neutron), so the reaction cross section is proportional to the probability of fining this nucleon in the deuteron with its final momentum. This probability is $|\Phi(p_n)|^2$, where $\Phi(p_n)$ is the Fourier transform of the deuteron wave function.

The spectator peaks were fitted by assuming that the cross section was proportional to the product of $|\Phi(p_n)|^2$ and the phase space factor.

$$\frac{d^3\sigma}{d\Omega_p d\Omega_\alpha dE_\alpha} = \frac{\text{constant}\cdot E_p\sqrt{E_\alpha}}{\left(\sqrt{E_p}+\sqrt{E_\alpha}\cos\theta_{\alpha p}-\sqrt{E_0}\cos\theta_p\right)\left(E_1+2E_n\right)^2\left(E_2+2E_n\right)^2}$$

The calculated cross sections are shown in figures 4 and 5 by solid curves. Arrows indicate the minimum laboratory neutron kinetic energies, where $|\Phi(p_n)|^2$ takes on its maximum value, and the calculated curves are normalized to the measured cross sections at these points.

The predicted peaks are correctly centered in the E_α spectra at $(\theta_\alpha, \theta_p)$ equal to $(9.8^o, 40^o)$ and $(14.8^o, 50^o)$. The $(14.8^o, 50^o)$ peak width is correctly predicted, but the $(9.8^o, 40^o)$ peak is inexplicably sharp. At forward proton scattering angles, the large width of the ^{5}Li ground state may contribute to the large yields observed on the high energy side of the spectator peaks, where typically $E_{\alpha p} \approx 3$ or 4 MeV. At $(\theta_\alpha, \theta_p)$ equal to $(9.8^o, 20^o)$, the combined effects of the spectator peak and the ^{5}Li FSI produced the largest measured cross section.

A question arises as to whether the measured cross section, integrated over detector solid angles, is accurately equal to the coplanar cross section which would be measured with a target and detectors of infinitesimal height. In general, E_n will increase and $|\Phi(p_n)|^2$ will decrease with increasing noncoplanarity. The increase in neutron energy will have its maximum value ΔE_n when the incident α strikes the top (bottom) of the target and each of the detected particles strikes the bottom (top) edge of its detector. If t and C are the half-heights of the beam spot and counters, respectively, and if L is the target-to-counter distance, it can be shown that

$$\Delta E_n \approx E_p \left[\frac{(t + C)(\sin \theta_\alpha + \sin \theta_p)}{L \sin \theta_\alpha} \right]^2$$

In this experiment, ΔE_n has its largest value of about 0.6 MeV in the spectator peak at $(\theta_\alpha, \theta_p)$ equal to $(9.8^o, 40^o)$, which would reduce $|\Phi(p_n)|^2$ by about a factor of two from its coplanar value. However, a realistic calculation of the effect of noncoplanarity, integrated over the beam spot and detector heights, suggests that the measured averaged cross section should be not less than about 90 percent of the coplanar cross section.

Helium 5 Final State Interactions

In the ^{5}He peaks in figures 4 to 6, the reaction is thought to proceed sequentially rather than by direct breakup. The alpha-particle first captures the neutron, forming ^{5}He in its ground state, and the ^{5}He then decays into α+n. It follows that these peaks will be observed when the relative energy of α+n in their center-of-mass system is equal to the excitation energy of the ^{5}He ground state (0.96 MeV). This relative energy, called $E_{\alpha n}$, is calculated from the equation

$$E_{\alpha n} = 0.2\,E_0 - D - 1.2\,E_p + 0.8\,(E_0 E_p)^{1/2} \cos\theta_p$$

Typically, $E_{\alpha n}$ may vary from a minimum of ~0.2 MeV at $E_\alpha \sim 20$ MeV to several MeV at the largest and smallest E_α's observed, therefore $E_{\alpha n}$ passes through the resonance energy on either side of this minimum and two peaks are observed. In other cases, the minimum $E_{\alpha n}$ exceeds 0.96 MeV and there are no FSI peaks. The equation for $E_{\alpha p}$, the relative energy of α+p in their center-of-mass system, is

$$E_{\alpha p} = 0.2E_\alpha + 0.8E_p - 0.8\,(E_\alpha E_p)^{1/2} \cos\theta_{\alpha p}$$

Arrows labelled ^{5}He are placed at those E_α's at which $E_{\alpha n} = 0.96$ MeV. Most of the FSI peaks are slightly displaced from these expected locations, and these displacements are caused, in part, by two effects:

(1) The 0.96 MeV energy corresponds to a 90° n-α phase shift, but penetration factors (ref. 2) shift the peaks in particle energy spectra to lower $E_{\alpha n}$.

(2) The arrow locations were calculated for coplanar events, and finite geometry effects shift the peaks toward each other.

These effects cannot fully account for the observed peak displacements since, for example, both of them shift the higher energy peak at (θ_α, θ_p) equal to (14.8°, 60°) in the wrong direction. Noncoplanarity effects should not affect the measured cross section (except for the unresolved peaks described in the next paragraph), even for the worst noncoplanar geometries, since $E_{\alpha n}$ ranges through the entire resonance region (about 0.6 to 1.3 MeV) near the FSI peaks.

For (θ_p, θ_α) equal to (19.8°, 20°) and (19.8°, 60°), the two possible ^{5}He FSI peaks are not resolved. This is expected, since, between the peaks, $E_{\alpha n}$ reaches minima of 0.5 and 0.8 MeV at $\theta_p = 20°$ and 60°, respectively. Thus, $|E_{\alpha n} - 0.96\ \text{MeV}|$ is approximately equal to or less than the width of the ground state (about 0.3 MeV HWHM).

From the seven largest resolved ^{5}He FSI peaks at $\theta_\alpha = 14.8°$ and 19.8°, a Q value of 0.88 ± 0.12 MeV is obtained for $^5\text{He} \rightarrow \alpha$+n, in agreement with the accepted value (ref. 8). A width of 0.75 ± 0.20 MeV for the ^{5}He ground state is also obtained.

Lithium 5 Final State Interactions

The peak at (θ_α, θ_p) equal to (14.8°, 10°) can be attributed to a p+α FSI through the ^{5}Li ground state since its excitation ($E_{\alpha p} = 1.9$ MeV) and width (1.4 MeV) are close to the accepted values (ref. 8). Other ^{5}Li FSI peaks at (θ_α, θ_p) equal to (14.8°, 20°) and (9.8°, 20°) cannot be safely analyzed because the resultant protons have energies

just above the detection threshold; an analysis of the latter peak would also be complicated by the proximity of the spectator pole peak.

CONCLUSION

The breakup of deuterons by 42 MeV alpha particles is dominated by both the final state interactions in the lithium 5 and helium 5 ground states and the quasi-elastic alpha-nucleon scattering with the second nucleon acting as a spectator.

Lewis Research Center,
National Aeronautics and Space Administration,
Cleveland, Ohio, June 21, 1967,
129-02-04-06-22.

REFERENCES

1. Warburton, E. K.; and McGruer, J. N.: Deuteron-Induced Reactions from N^{14}, N^{15}, and He^4. Phys. Rev., vol. no. 2, Jan. 15, 1957, pp. 639-647.

2. Ohlsen, G. G.; and Young, P. G.: Protons from the Deuteron Bombardment of Helium-4. Phys. Rev., vol. 136, no. 6B, Dec. 21, 1964, pp. 1632-1639.

3. Nagatani, K.; Tombrello, T. A.; and Bromley, D. A.: Alpha-Particle-Induced Breakup of the Deuteron. Phys. Rev., vol. 140, no. 4B, Nov. 22, 1965, pp. 824-834.

4. Goulding, Fred S.; Landis, Donald A.; Cerny, Joseph, III; and Pehl, Richard H.: A New Particle Identifier Technique for Z = 1 and Z = 2 Particles in the Energy Range > 10 MeV. IEEE Trans. on Nucl. Sci., vol. NS-11, no. 3, June 1964, pp. 388-398.

5. Broek, H. W.; and Yntema, J. L.: Plastic Scattering of 21.0 - MeV Deuterons by He^4. Phys. Rev., vol. 135, no. 3B, Aug. 10, 1964, pp. 678-679.

6. Kuckes, A. F.; Wilson, R.: and Cooper, P. F., Jr.: On Deuteron as Free Nucleon Target at 145 MeV. Ann. Phys. (N.Y.), vol. 15, no. 2, Aug. 1961, pp. 193-222.

7. Burress, David A.: Theoretical Alpha-Deuteron Cross Section by Simple Approximation. B. A. Honors Thesis, Oberlin College, 1966.

8. Lauritsen, T.; and Ajzenberg-Selove, F.: Energy Levels of Light Nuclei (VII). A = 5 - 10. Nucl. Phys. vol., 78, 1966, pp. 1-176.

"The aeronautical and space activities of the United States shall be conducted so as to contribute . . . to the expansion of human knowledge of phenomena in the atmosphere and space. The Administration shall provide for the widest practicable and appropriate dissemination of information concerning its activities and the results thereof."

—NATIONAL AERONAUTICS AND SPACE ACT OF 1958

NASA SCIENTIFIC AND TECHNICAL PUBLICATIONS

TECHNICAL REPORTS: Scientific and technical information considered important, complete, and a lasting contribution to existing knowledge.

TECHNICAL NOTES: Information less broad in scope but nevertheless of importance as a contribution to existing knowledge.

TECHNICAL MEMORANDUMS: Information receiving limited distribution because of preliminary data, security classification, or other reasons.

CONTRACTOR REPORTS: Scientific and technical information generated under a NASA contract or grant and considered an important contribution to existing knowledge.

TECHNICAL TRANSLATIONS: Information published in a foreign language considered to merit NASA distribution in English.

SPECIAL PUBLICATIONS: Information derived from or of value to NASA activities. Publications include conference proceedings, monographs, data compilations, handbooks, sourcebooks, and special bibliographies.

TECHNOLOGY UTILIZATION PUBLICATIONS: Information on technology used by NASA that may be of particular interest in commercial and other non-aerospace applications. Publications include Tech Briefs, Technology Utilization Reports and Notes, and Technology Surveys.

Details on the availability of these publications may be obtained from:

SCIENTIFIC AND TECHNICAL INFORMATION DIVISION

NATIONAL AERONAUTICS AND SPACE ADMINISTRATION

Washington, D.C. 20546